energies

MDPI

Article

Calculation of the Shading Factors for Solar Modules with MATLAB

Martín Silva, Justo Jose Roberts * and Pedro Osvaldo Prado

Research and Development Group on Geotechnologies and Energy, Engineering Faculty, National University of Mar del Plata (UNMdP), Av. Juan B. Justo 4302, Mar del Plata, Buenos Aires B7608FDQ, Argentina; martinsilva.ing@gmail.com (M.S.); poprado@fi.mdp.edu.ar (P.O.P.)

* Correspondence: jjroberts@fi.mdp.edu.ar; Tel.: +54-9-(2262)-488400

Abstract: Shadows severely affect the performance of solar photovoltaic (PV) systems. A proper description of this effect is useful for sizing and simulating PV systems when shadows cannot be avoided. Shading factors represent the basis for simulating the effect of shadows on solar modules. These factors can be used to estimate shading losses, calculate their I-V and P-V curves under shading conditions, or develop new maximum power point tracking (MPPT) techniques. Open-source libraries focused on solar energy have gained popularity in recent years. One of the currently most popular ones is the PV_LIB toolbox initially developed by Sandia Laboratories. PV_LIB significantly facilitates solar energy calculations. However, it currently lacks functions for taking into account shaded conditions. In this paper, a detailed Matlab-based method for calculating the shading factors is provided. The method has been used for elaborating a toolbox for shading calculations. The current work could help extend the functionalities of the PV_LIB toolbox. The results were compared against other currently popular computer programs, namely the System Advisor Model (SAM) and PVsyst. With this method, it is also possible to calculate shading factors with smaller time steps than possible with the mentioned programs. This work also shows the importance of using small time steps and how this can affect the accuracy of the calculated shading factors. The contribution of this work is providing a way of quantifying shadow losses in PV systems with Matlab, allowing for better accuracy, flexibility, and transparency during the calculation. The functions developed in this work can be accessed by contacting the authors.

Keywords: solar; shadows; Matlab; SAM; PVsyst

check for updates

Citation: Silva, M.; Roberts, J.J.; Prado, P.O. Calculation of the Shading Factors for Solar Modules with MATLAB. *Energies* **2021**, *14*, 4713. https://doi.org/10.3390/en14154713

Academic Editor: Acha-Daza Enrique

Received: 9 June 2021
Accepted: 26 July 2021
Published: 3 August 2021

Publisher's Note: MDPI stays neutral with regard to jurisdictional claims in published maps and institutional affiliations.

Copyright: © 2021 by the authors. Licensee MDPI, Basel, Switzerland. This article is an open access article distributed under the terms and conditions of the Creative Commons Attribution (CC BY) license (https://creativecommons.org/licenses/by/4.0/).

1. Introduction

With the reduction of solar energy costs, government initiatives in many countries and a general trend toward renewable energies, the use of solar photovoltaic (PV) systems in urban and residential environments has greatly increased [1–7]. Urban environments often include obstacles that could cast shadows on a PV system, badly affecting energy production. In Germany, studies have shown that shading is one of the main causes of a lower energy yield [8]. Results from the German 1000 Roofs Programme in 1990 revealed shading losses of up to 10% in more than half of their PV systems [4,8,9]. More recently, an analysis of 46 residential PV systems in the United States showed that annual shading losses can account for up to 20% [10]. Bayrak et al. [11] conducted an experiment where they applied different shading ratios to a single module. They analyzed three shading configurations: namely, shading of a single cell, horizontal shading of a row of cells, and vertical shading of a column of cells. The study showed that horizontal shading can completely reduce the power yield of a module when all by-pass diodes are affected, while single-cell shading and vertical shading presented reductions of 69.92% and 66.93% respectively. More recently, Numan et al. [12] investigated theoretically and experimentally the impacts of various cases of partial shading (vertical string, horizontal string, and single cell) on the performance of a photovoltaic system. The authors found that at the

100% shading condition, the maximum power dropped by 99.36%, 43.7%, and 41.15% for horizontal, cellular, and vertical shading at the same solar radiation level compared to their initial state values.

Limited space in urban areas and the inability to avoid or remove obstacles demand a method for including their effects in the PV system design phase. The reduction of global irradiance due to shadows can be computed with shading factors that reduce its components linearly [13]. The electrical effect needs to be computed with mathematical models of the solar module, such as the one-diode or two-diode model [14,15]. This can be computationally expensive, and some authors have proposed using look-up tables with pre-calculated values to speed up calculations [16]. In this paper, the main focus is on the global irradiance reduction and the computation of shading factors.

Even though shading factors have been used for more than 25 years, the number of articles on this topic is limited. In 1995, Quaschning and Hanitsch [13] proposed the use of shading factors and a vectorial approach, where the module, the obstacle, and the sun are represented as vectors. This allowed one to easily calculate the shadows projected on the surface of a PV array. In 2011, Cascone et al. [17] presented a similar procedure for the calculation of the shading factors. Although this work was meant for the study of heat gain in buildings, the principle of the factor is the same as for solar modules. The procedure is very similar to the one proposed by Quaschning. However, it is much more detailed. Melo et al. [18] developed an add-in for SketchUp that can be used for calculating a table of direct shading factors and the diffuse shading factor as well. Their approach is the same used by Quaschning and Cascone. With SketchUp, they can analyze shading situations with complex geometries. Westbrook et al. [19] modeled diffuse shading losses with an analytical approach based on an isotropic sky. They limited their study to an array being shaded by another array of unlimited length and compared the results to experimental data. Li et al. [20] proposed a pixel-based methodology to assess the annual solar potential of building rooftops. In this work, the authors used SketchUp to extract images depicting a certain shading situation and then processed the images with Matlab.

Currently, many computer programs use shading factors when calculating shadow losses. The most popular ones are SAM [21], PVsyst [22], PV*SOL [23], and Helioscope [24]. Another option currently gaining more popularity is the PV_LIB library provided by Sandia National Laboratories [25]. This library is free and available for both Matlab and Python. It has many functions that greatly facilitate the simulation of solar modules. Despite this, there are currently no functions in this library for the inclusion of shading losses. The present work could help extend the PV_LIB Matlab library functions to include shadow losses. Matlab has been widely used for shading calculations [26]; therefore, the idea of including a Matlab-based tool for estimating shading losses is very attractive.

This paper provides a detailed and simple procedure for calculating the shading factors for both the direct and diffuse components. The procedure was implemented in Matlab, and the results were compared with SAM and PVsyst.

2. The Shading Factors

The usual approach for introducing the effect of shadows on the solar modules is including shading factors. These factors work by reducing the irradiance reaching the surface of the module. They take values from 0 (absence of shadow) up to 1 (fully shaded). The factors f_B and f_D are the direct and diffuse shading factors, respectively. The direct shading factor depends on the geometry of the modules, obstacles, and the position of the sun. The diffuse shading factor depends solely on the geometry of the modules and obstacles. Obstacles also reduce the reflected component, and this is usually taken into account by reducing the albedo [13]. However, this effect is out of the scope of this work. The reduced direct and diffuse irradiances can be calculated with Equations (1) and (2) [13]. DNI is the direct normal irradiance and DHI the diffuse horizontal irradiance, while the subindex S stands for shaded.

$$\mathrm{DNI_S} = \mathrm{DNI} \cdot (1 - f_B) \quad (1)$$

$$\mathrm{DHI_S} = \mathrm{DHI} \cdot (1 - f_D) \tag{2}$$

To calculate these factors, we first calculate f_B with a vectorial approach. Then it is necessary to compute all the f_B into a table where the rows correspond to sun elevation angles and the columns to sun azimuth angles, going from 0° to 90° and -180° to 180°, respectively. This table has two main purposes. First, it will serve as a look-up table when calculating factors for all the given sun positions throughout a year. Second, f_D can be calculated by integrating the values in this table. The methodology for creating the shading table is illustrated in Figure 1.

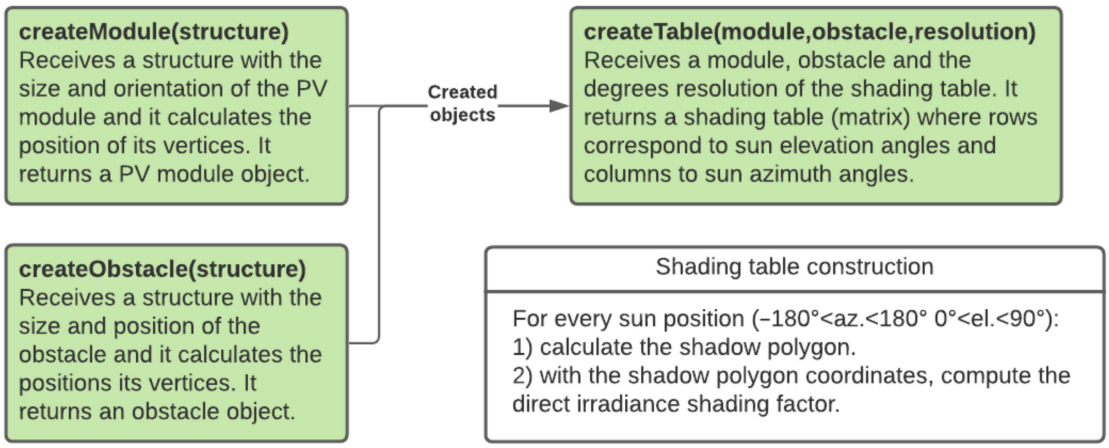

Figure 1. The classes createModule and createObstacle are used for creating the PV module and obstacle objects. The objects contain the geometry of the given situation. The class createTable receives the module, obstacle, and the angle resolution of the sun elevation and azimuth angles. Finally, the class returns a shading table object.

2.1. Direct Irradiance Shading Factor

The direct shading factor f_B is defined as the ratio between the shaded area A_S and the area of the module A_M, as shown in Equation (3) [13]. When the shadow covers the module entirely, A_S is equal to A_M and f_B is 1. Contrarily, when there is no shadow, A_S and f_B are 0.

$$f_B = \frac{A_S}{A_M} \tag{3}$$

To calculate this factor, it is necessary to calculate the area of the shadow A_S. First, the geometry of both the solar module and the obstacle needs to be specified. Second, the vertices of the obstacle are projected onto the plane defined by the solar module. Third, a convex hull procedure is applied to the projected points. Finally, we subtract the part of the projected shadow that falls outside the module to obtain A_S and calculate f_B. The final step will be making a shading table [27].

2.1.1. Module Geometry Definition

The module is represented with four Cartesian coordinates. These coordinates correspond to the vertices of each corner of the module. This was implemented as a class that receives a structure with the dimensions of the module, its coordinates, and its orientation angles. The constructor of this class calculates the coordinates for the four vertices that represent the module. Figure 2 shows the four vertices v_i of a module facing north (positioned on the southern hemisphere). Azimuth angles are measured from north and positive clockwise (West = 270°).

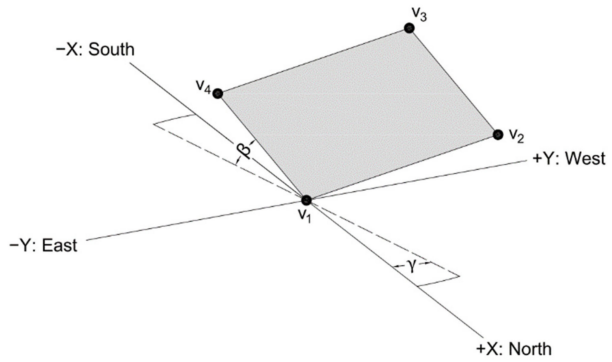

Figure 2. Geometric definition of the vertices v_1, v_2, v_3, and v_4 for a solar module with tilt angle β and azimuth angle γ. Azimuth angles are measured from north and positive clockwise.

The initial coordinates of the four vertices are given by:

$$v_1 = (0, 0, 0)$$

$$v_2 = (0, \text{width}, 0)$$

$$v_3 = (\text{length}, \text{width}, 0)$$

$$v_4 = (\text{length}, 0, 0)$$

Then, each vertex v_i is placed on its final position performing two rotations and one translational displacement. The two rotations are performed by multiplying each vertex coordinate by a rotation matrix. The first rotation is about the y axis and corresponds to the tilt angle β of the module. The second rotation is about the z axis and corresponds to the azimuth angle γ of the module. The translational displacement is simply performed by adding the displacement vector D to each vertex coordinate. This calculation is shown in Equation (4).

$$v_i = R_y(\beta) \cdot R_z(\gamma) \cdot \begin{pmatrix} v_x \\ v_y \\ v_z \end{pmatrix} + D \tag{4}$$

where R_y and R_z are the rotation matrixes. The expressions for R_y and R_z are shown in Equations (5) and (6), respectively [28].

$$R_y(\beta) = \begin{bmatrix} \cos\beta & 0 & \sin\beta \\ 0 & 1 & 0 \\ -\sin\beta & 0 & \cos\beta \end{bmatrix} \tag{5}$$

$$R_z(\gamma) = \begin{bmatrix} \cos\gamma & -\sin\gamma & 0 \\ \sin\gamma & \cos\gamma & 0 \\ 0 & 0 & 1 \end{bmatrix} \tag{6}$$

2.1.2. Obstacle Geometry Definition

We limited this study to obstacles modeled as rectangular prisms. Other, more complex geometries could be included in future works. In a similar way to the module, the prism is represented with eight Cartesian coordinates, each representing one of its corners. This was done with a class that receives the dimensions of the obstacle, its position, one tilt angle, and one azimuth angle. Figure 3 shows the 3D output generated in Matlab. For more than one obstacle, they must be created and saved in a vector array of obstacle objects.

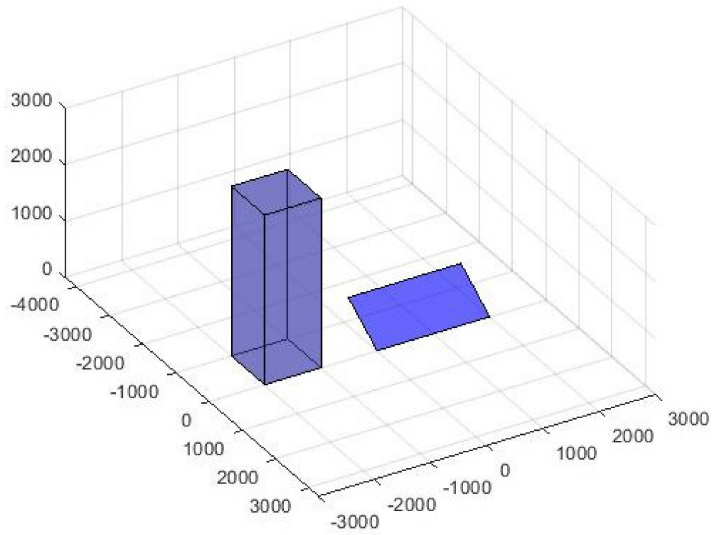

Figure 3. Visual output of one module with one obstacle generated in Matlab.

2.1.3. Shadow Calculation Procedure

The goal of this step is obtaining the coordinates of the projected shadow. This is done by projecting each vertex of the obstacle onto the plane given by the module. The coordinates of the projections can be calculated as the intersection of a line (defined by the obstacle vertex p_0) and a plane (defined by the module). Quaschning provides Equation (7) based on this principle [13], where a is a vector perpendicular to the module, p_0 is a vertex of the obstacle, p_s is the projection of p_0 on the plane defined by the module, and s is a unit vector indicating the position of the sun. Figure 4 shows one projected vertex of the obstacle on the surface of the module. Vectors v_i are the corners of the module.

$$p_s = p_0 - \left[\frac{a \cdot (p_0 - v_1)}{a \cdot s}\right].s \tag{7}$$

$$a = (v_4 - v_1) \times (v_2 - v_1) \tag{8}$$

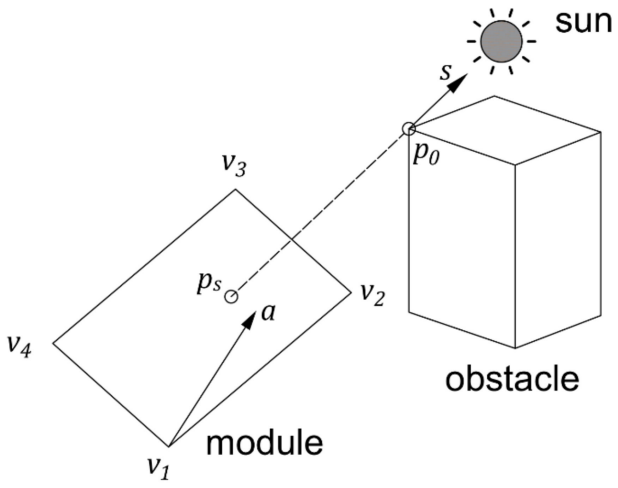

Figure 4. A vertex p_0 of one obstacle is projected on the plane defined by the module. The projected point is called p_s. The vector s is a vector pointing towards the sun. The vector a is normal to the plane of the module. v_1, v_2, v_3, and v_4 are the positions of the vertices that define the module.

It is important to notice that when $a \cdot s < 0$, the sun will be behind the surface of the module. Knowing when the sun is behind the surface of the module will be helpful when estimating the diffuse shading factor.

On the other hand, vertices behind the module will also have projections on the plane. This will have no physical sense and therefore, these vertices need to be removed. If part of an obstacle is behind the module, the obstacle will have to be sliced. This procedure can be complex because it will lead to a new shape with new vertices. However, one simple approach that works for not-tilted rectangular prisms is moving the points that are behind the plane vertically onto the plane (see Figure 5).

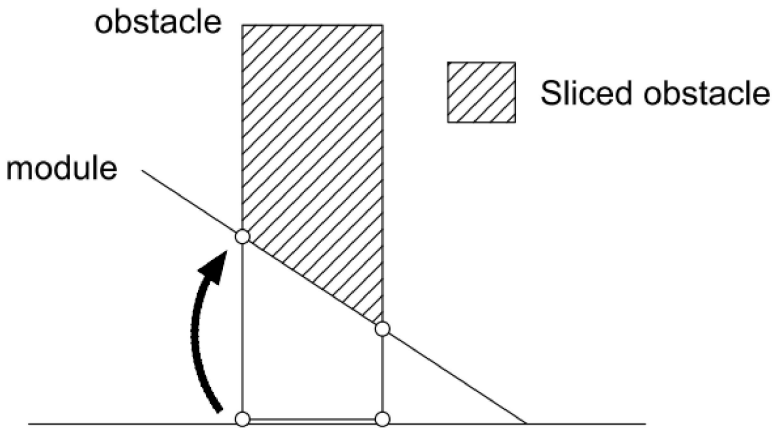

Figure 5. Side view of one module and one obstacle. If some of the obstacle vertices are behind the module plane, it is possible to slice the obstacle by moving these vertices vertically until they are positioned on the plane.

The module defines the plane given by Equation (9), where a_x, a_y, a_z are the components of the unit vector normal to the module surface and d is a constant [29]. The new z coordinate of the obstacle vertices behind the surface will be given by Equation (10).

$$x a_x + y a_y + z a_z + d = 0 \tag{9}$$

$$p_{o,z} = -\left(a_x p_{o,x} + a_y p_{o,y} + d\right) / a_z \tag{10}$$

where $p_{o,x}$, $p_{0,y}$, and $p_{o,z}$ are the x,y, and z coordinates of the obstacle vertex, respectively.

After projecting all the vertices on the plane, a convex hull procedure needs to be applied. The reason is that not all projected vertices will correspond to shadow vertices (see Figure 6). This is easily done in Matlab with the convhull function [30].

First, we temporarily remove the z coordinate of the projected points. Then, we apply the convhull function, retrieve the points that correspond to the shadow, and finally include the z coordinates again. The result is shown in Figure 7.

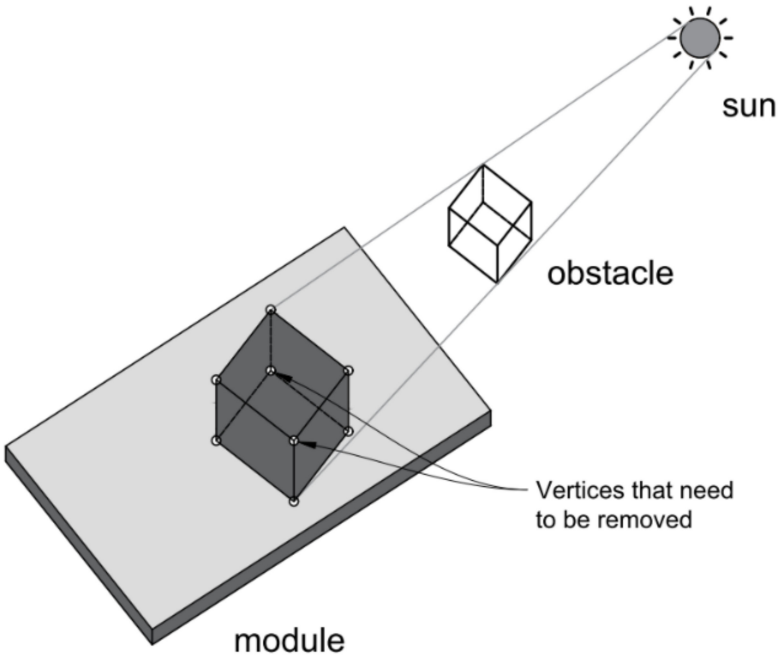

Figure 6. Projection of each of the eight obstacle vertices onto the surface of the module. After projecting all the points, there are two points that need to be removed. These two points are internal to the shadow and do not correspond to the ones located on the perimeter of the shadow.

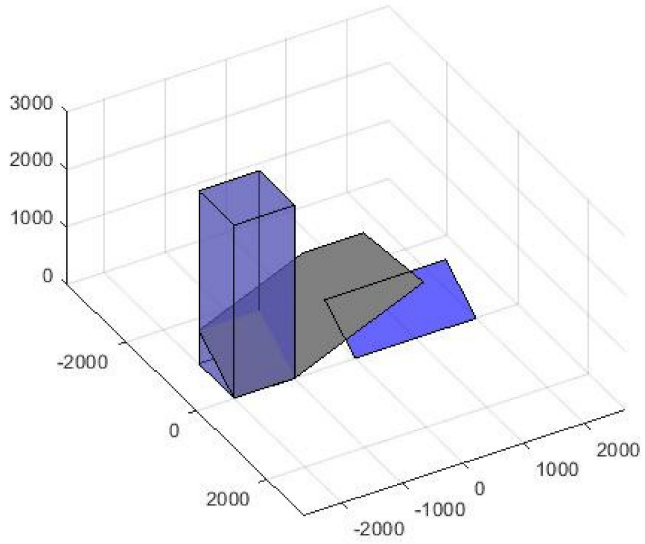

Figure 7. Visual output of one module and one obstacle casting a shadow on the plane defined by the module.

2.1.4. Shading Factor Calculation

The final step is to crop the resulting shadow to calculate the portion that falls on the surface of the module. First, we remove the z coordinate from the module vertices and the shadow vertices. This will flatten both the module polygon and the shadow polygon on the $x - y$ plane. Then, we can convert these 2D polygons into polyshape objects [31] and find the intersection of the shadow with the module with the intersect function [32]. The result is another polygon A_S that represents the shadow falling on the module as shown in Figure 8.

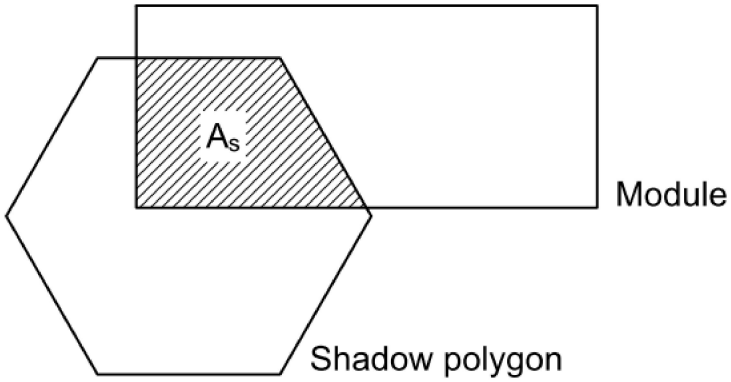

Figure 8. Area of the shadow that falls on the surface of the module. The previously calculated shadow polygon must be cropped in order to find the portion of shadow that falls on the module (A_s, hatched area).

Finally, we compute the shadow factor as the ratio between the intersected shadow area A_s and the area of the module polygon A_M with Equation (11).

$$f_B = \frac{A_S}{A_M} \tag{11}$$

2.1.5. Shading Table

The shading table is a matrix of shading factors for the direct component [27]. The columns correspond to sun azimuth angles and the rows to sun elevation angles. The advantage of using a table is calculating a set of shading factors once, and then using this matrix to retrieve the factors as needed. Apart from this, the table is helpful when calculating the diffuse shading factor by the integration of its values. In our approach, we calculated the shading factors for all azimuth angles from −180° to +180° and elevation angles from 0° to 90°. This can be done in 5-degree steps and by later interpolating the results for a 1-degree resolution. The resulting table will have a similar structure to the one shown in Table 1. Figure 9 is a heat plot that illustrates the high-resolution shading table. The white portions in the bottom corners correspond to sun positions behind the module (NaN values). It is very important to include these points and clearly distinguish them from the rest. Blue spots correspond to low shading factor values, while yellow spots correspond to shading factors closer to 1.

Table 1. Simplified version of the shading table for an arbitrary situation.

Elevation\Azimuth	−150	−100	−50	0	50	100	150
0	NaN	NaN	NaN	1.00	NaN	NaN	NaN
10	NaN	0.00	0.86	0.92	0.86	0.00	NaN
20	NaN	0.20	0.74	0.82	0.74	0.20	NaN
30	0.00	0.30	0.66	0.74	0.66	0.30	0.00
40	0.00	0.34	0.61	0.68	0.61	0.34	0.00
50	0.01	0.37	0.56	0.62	0.56	0.37	0.01
60	0.19	0.39	0.52	0.57	0.52	0.39	0.19
70	0.29	0.40	0.49	0.52	0.49	0.40	0.29
80	0.37	0.41	0.46	0.48	0.46	0.41	0.37
90	0.42	0.42	0.42	0.42	0.42	0.42	0.42

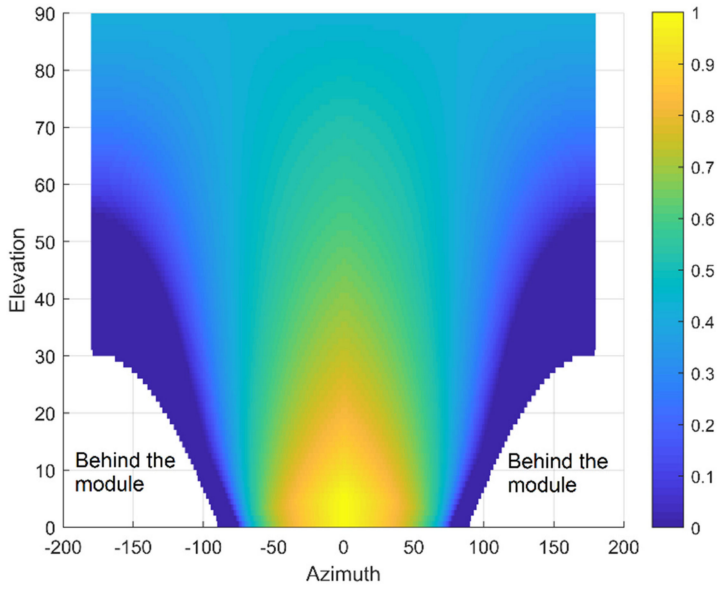

Figure 9. Heat map representation of the shading table. Yellow portions correspond to higher shading factors for the direct irradiance. Blue values correspond to low shading factors for the direct irradiance. The white parts on the bottom left and right corners of the heat map correspond to angles where the sun is behind the module (NaN values).

2.2. Diffuse Shading Factor

The diffuse shading factor f_D is constant throughout the year and for a fixed geometry needs to be determined only once [13]. If we consider an imaginary hemisphere surrounding the module, a nearby obstacle will block the sun on the area $A_S \cdot f_D$ can be defined as the ratio between the irradiance I_S that traverses the shaded area A_S and the irradiance I_H reaching the portion of the hemisphere A_H in front of the module as shown in Figure 10. The expression for f_D is given by Equation (12) [13].

$$f_D = \frac{I_S}{I_H} \tag{12}$$

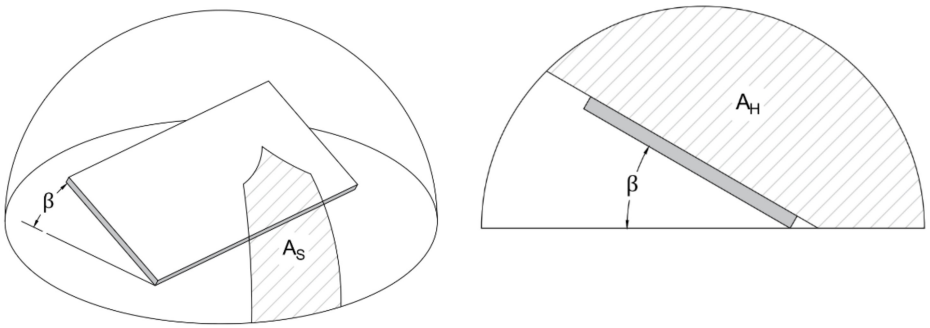

Figure 10. Calculation of the shading factor for the diffuse irradiance. If the solar module is covered by an imaginary hemisphere, then one nearby obstacle will reduce the diffuse irradiance reaching this hemisphere. A_S is the portion of the hemisphere where the sun is blocked by the obstacle. The diffuse irradiance shading factor is given as the ratio between the irradiance traversing A_S and the irradiance traversing the hemisphere A_H.

The diffuse shading factor can also be calculated with Equation (13) [17], where R is the radiance of a sky element and AOI is the angle of incidence [33]. The angle of incidence is the angle between the vector normal to the array and the sun position. It is calculated

with Equation (14). To account only for the radiance component normal to the array, the cosine of the angle of incidence is applied [19]. The integration region is limited by all the points of the hemisphere that are in front of the module plane [9].

$$f_D = \frac{\iint f_B \cdot R \cdot \cos(\mathrm{AOI}) \cdot \cos(\alpha) \cdot d\alpha \cdot d\gamma}{\iint R \cdot \cos(\mathrm{AOI}) \cdot \cos(\alpha) \cdot d\alpha \cdot d\gamma} \tag{13}$$

$$\mathrm{AOI} = \cos^{-1}\left[\sin(\alpha)\cos(\beta) + \cos(\alpha)\sin(\beta)\cos\left(\gamma - \gamma_{array}\right)\right] \tag{14}$$

The $\cos(\alpha)$ factor takes into account that the hemisphere subdivisions are smaller when the elevation angle is closer to 90° [34]. If an isotropic sky is considered, the radiance R can be removed from the integrals and cancelled. Moreover, if the sky is discretized, the values of the previously calculated shading table can be used. The calculated table has a resolution of 1 degree for both the altitude and azimuth angles, going from 0° to 90° and −180° to 180°, respectively. Therefore, the table has 91 × 361 elements. Finally, Equation (13) is simplified into Equation (15). The NaN values will not add up to each summation.

$$f_D = \frac{\sum_{i=1}^{91}\sum_{j=1}^{361} f_{B_{ij}} \cdot \cos\left(\mathrm{AOI}_{ij}\right) \cdot \cos(\alpha_i)}{\sum_{i=1}^{91}\sum_{j=1}^{361} \cos\left(\mathrm{AOI}_{ij}\right) \cdot \cos(\alpha_i)} \tag{15}$$

2.3. PV Array Class

More complex shading situations can be simulated with the use of a PV array class. The inputs are the previously created module object, number of rows, number of PV modules per row, row spacing in millimeters, and the azimuth angle of the array. This class makes an array of modules and calculates all the coordinates and vertices from each module composing the array. Figure 11 shows the visual output of one array composed by 3 rows of 4 modules each, separated by 2 m and a tilt angle of 30°.

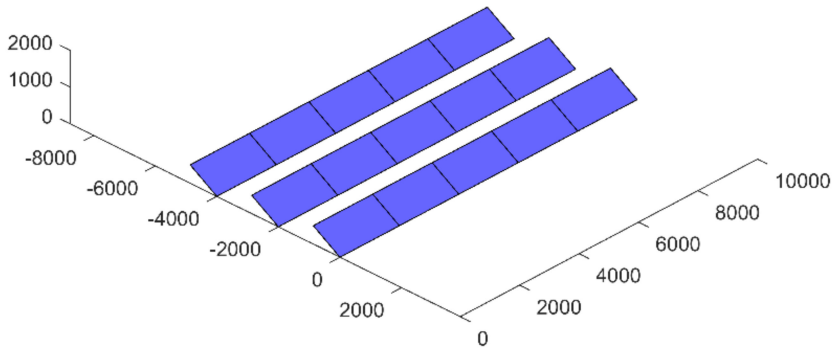

Figure 11. Visual output of a PV array modeled in Matlab.

This class has its own method for the computation of the shading table. The procedure for calculating the shading table is the same as previously explained, with the only difference that this method takes into account the shading between rows. To add the inter-row shading effect, it is only necessary to calculate f_B. for each module from the second row of the array. We know that the inter-row shading factors will be the same for all the rows behind because the distances of separation between rows are the same. Therefore, after calculating the factors for the second row we only have to replicate these values for the rows behind. The first row will not be affected by inter-row shading. For the inter-row shading calculation, each module is shaded by one rectangular obstacle with the dimensions of the row in front of it. For example, the first module of the second row will be shaded as illustrated in Figure 12. After calculating the shading tables for each module, the final result will be a cell array where each cell contains the shading table for each module. The used class was named createPVarray and its inputs are a module object, the number of rows of the array, number of columns, row spacing, and the azimuth angle of the array.

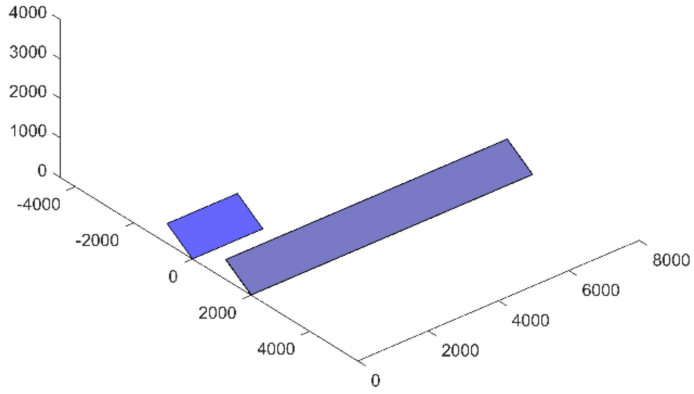

Figure 12. First module of the second row being shaded by the row in front. The shading factor for the inter-row shading is calculated for each module of the second row, being shaded by an obstacle with the size of the row in front.

3. Validation

The proposed tool was validated against two widely used PV simulation programs, SAM and PVsyst. First, we compare the resulting shading factors for the direct component and then for the diffuse component. To achieve this goal, two different shading situations with one single module and one obstacle are proposed. The first situation is a single module shaded by a rectangular block of $1 \times 1 \times 5$ m with 2 m of separation placed on the east side of the module (situation 1). The second situation consists of a module shaded by an infinite row of modules in front of it separated by 2 m (situation 2). The size of the module is 1×2 m, its tilt angle 30°, and the azimuth angle 0°. For the validation of the diffuse factor, we compared the results for different distances of separation in both situations. Figures 13 and 14 show the 3D geometry of the proposed situations and the heat plots for the shading tables calculated in Matlab. The geometry parameters are summarized in Table 2. It is important to emphasize that because the shading factors depend only on the time, location, and geometry of the given situation, other parameters are not needed to calculate the shading factors. Moreover, these shading situations were chosen due to their simplicity. After performing this validation with situations 1 and 2, a more complex shading simulation will be performed.

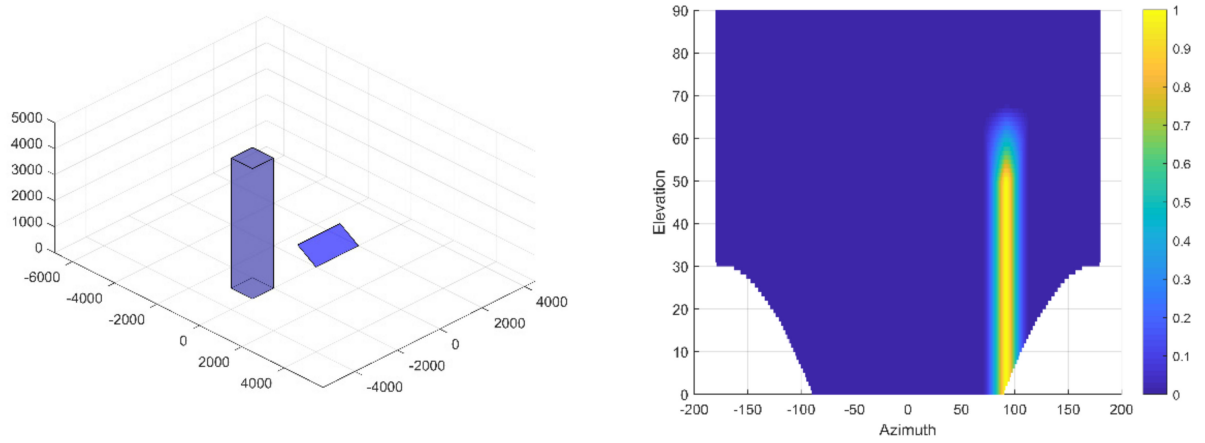

(**a**) (**b**)

Figure 13. Situation 1, one PV module being shaded by one obstacle positioned on its east side with 2 m of separation. The tilt angle of the module is 30° and the azimuth angle is 0°: (**a**) Visual output; (**b**) Heat plot representation of the shading table.

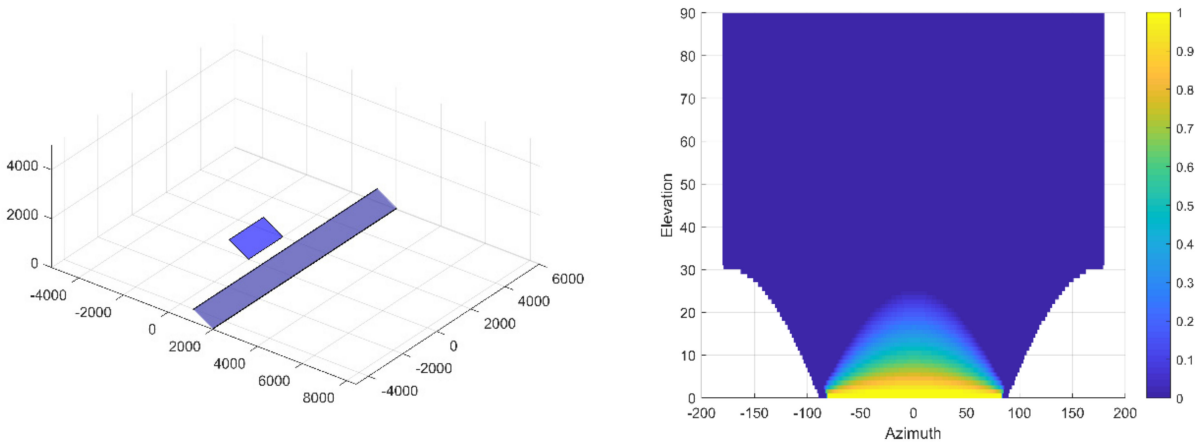

(**a**) (**b**)

Figure 14. Situation 2, one PV module being shaded by one infinite row in front. The tilt angle of the row is 30° and is positioned at 2 m from the module. The tilt angle of the module is 30° and the azimuth angle is 0°: (**a**) Visual output; (**b**) Heat plot representation of the shading table.

Table 2. Geometric parameters of the obstacle and the module for the proposed situations.

Parameters	Situation 1 (East Obstacle)	Situation 2 (Infinite Row)
	Obstacle Geometry	
Width (m)	1	30
Length (m)	1	0.05
Height (m)	5	1
Tilt angle (°)	0	60
Azimuth angle (°)	0	0
Distance of separation from module (m)	2	2
	Module Geometry	
Width (m)	2	
Height (m)	1	
Tilt angle (°)	30	
Azimuth angle (°)	0	

3.1. Direct Irradiance Shading Factor

We computed the f_B values for an entire year (2020) in Mar del Plata, Argentina (latitude −38°, longitude −57.5°, UTC-3). Figures 15 and 16 show the results for a single day for situations 1 and 2, respectively. In principle, the results of the three models agree thoroughly. The values of PVsyst had to be retrieved from the 3D geometry interface, where 5-min time steps are available. This is because currently PVsyst is limited to annual outputs with hourly steps, and the only way of retrieving factors with higher resolution is through the 3D geometry interface.

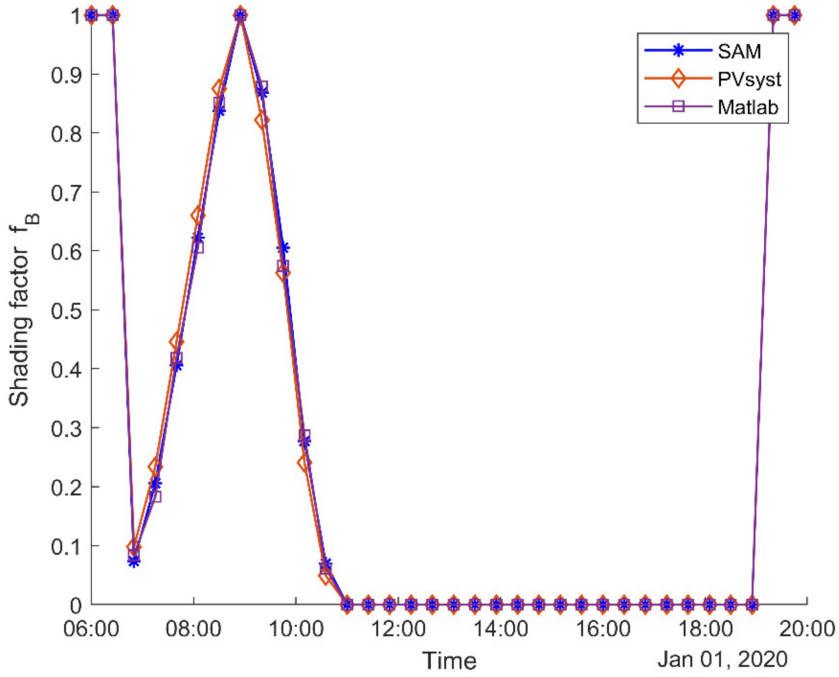

Figure 15. Shading factor f_B for situation 1 calculated for one day (1 January). f_B was calculated with the System Advisor Model (SAM), PVsyst, and the proposed Matlab tool.

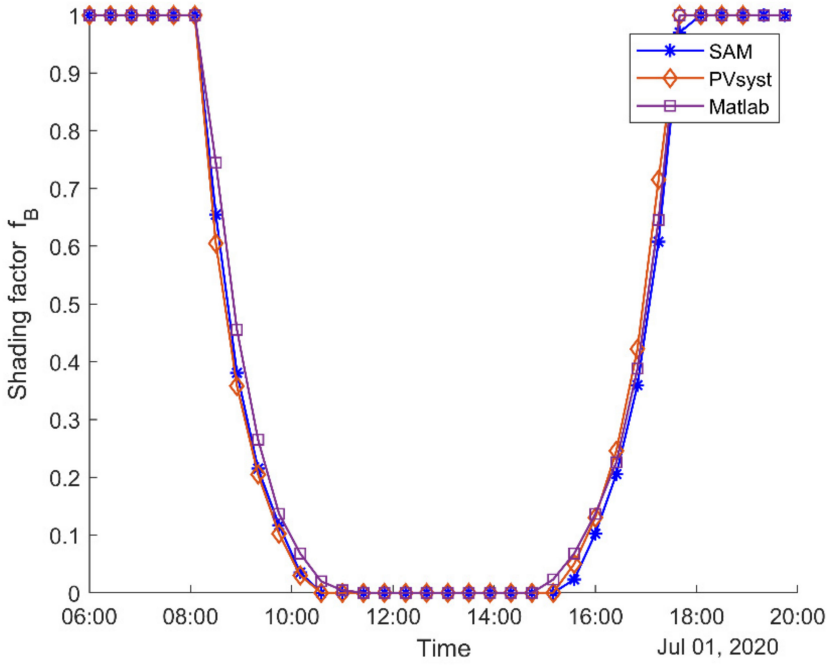

Figure 16. Shading factor f_B for situation 2 calculated for one day (1 July). f_B was calculated with the System Advisor Model (SAM), PVsyst, and the proposed Matlab tool.

When comparing the shading factors, hourly values had to be considered. Even though our model and SAM allow for smaller time steps, PVsyst is currently limited to hourly outputs. The effect of using different time steps is illustrated in Figure 17, where we calculate the shading factor with the Matlab tool for situations 1 and 2. The used time steps were 5 min, 30 min, and 1 h. It can be seen that as the magnitude of the steps increases, the shape of the figures deteriorates and loses symmetry.

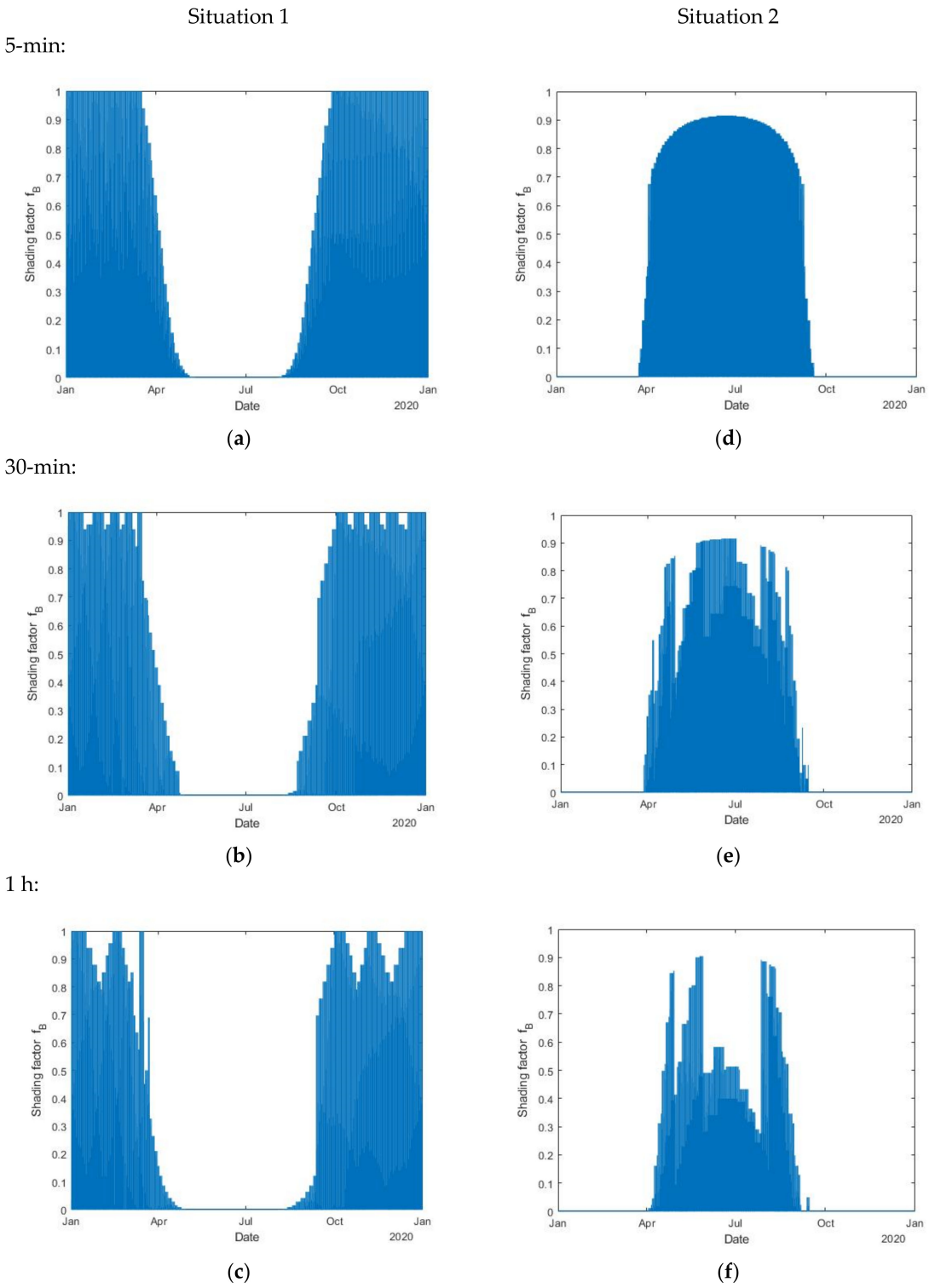

Figure 17. Effect of using different time steps when calculating the shading factor f_B with Matlab. For situation 1: (**a**) 5 min; (**b**) 30 min and (**c**) 1 h. For situation 2: (**d**) 5 min; (**e**) 30 min and (**f**) 1 h. As the time step increases, the yearly curve of f_B deteriorates and loses symmetry.

The f_B factors calculated with each program and with hourly time steps are shown in Figure 18. The first column corresponds to situation 1 and the second column to situation 2. Small differences can be seen in the shape of each figure. The greatest differences appear to be in the PVsyst results for situation 2.

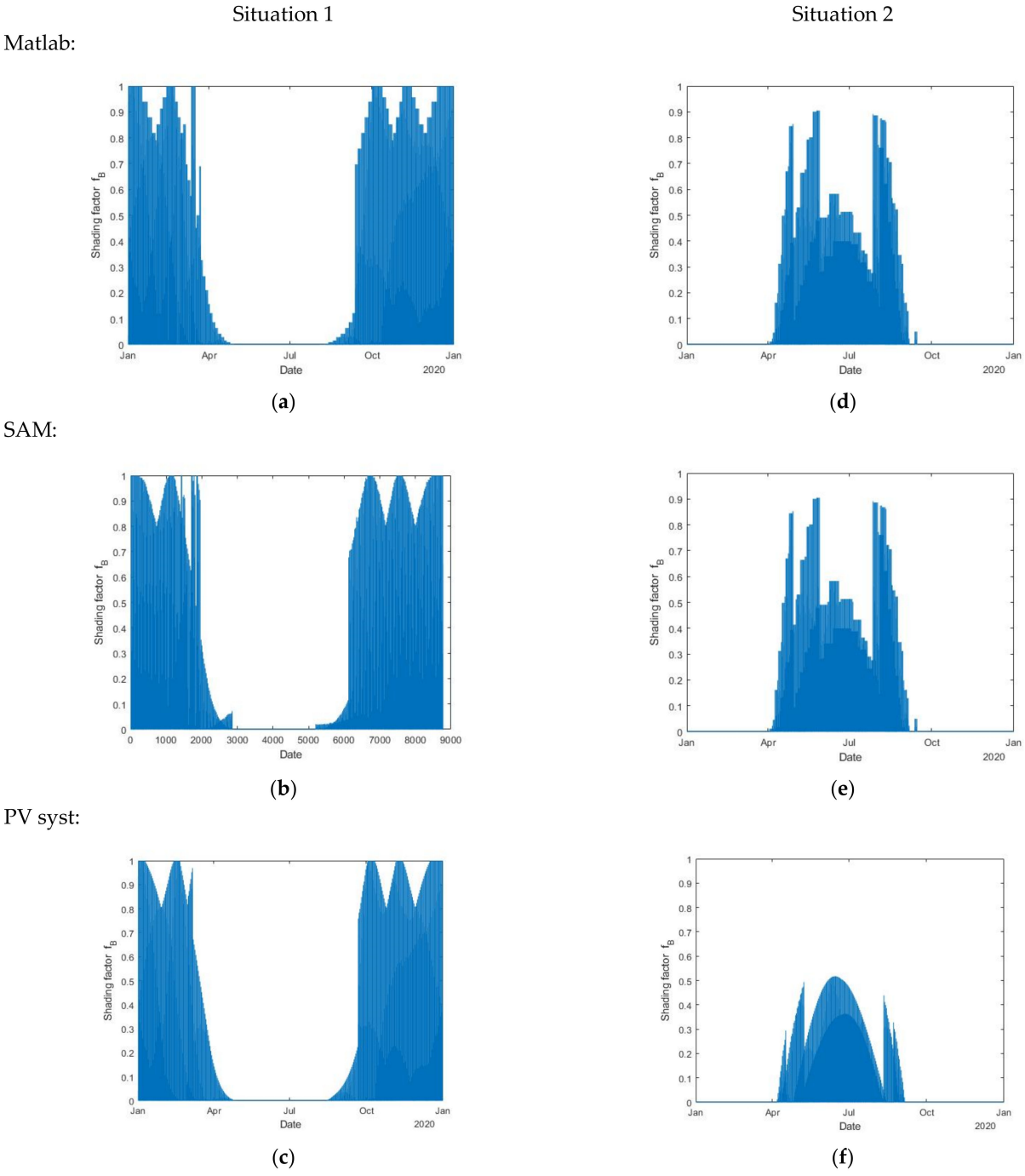

Figure 18. Shading factors f_B for a complete year. Results for situation 1 obtained with: (**a**) Matlab; (**b**) SAM and (**c**) PVsyst. Results for situation 2 obtained with (**d**) Matlab; (**e**) SAM and (**f**) PVsyst.

The monthly mean bias error (MBE) and the root mean square error (RMSE) were calculated. The results for situation 1 are shown in Table 3. Because in this particular condition the shading factor is zero from May to August, these months were excluded. The direct irradiance shading factors calculated with the Matlab tool had good correlation with both SAM and PVsyst. The scatter plots in Figure 19 illustrate the comparison between our model, SAM, and PVsyst.

Table 3. Deviation parameters between the Matlab tool, SAM, and PVsyst for situation 1.

East Obstacle								
Month	**SAM**				**PVsyst**			
	MBE	**MBEr (%)**	**RMSE**	**RMSEr (%)**	**MBE**	**MBEr (%)**	**RMSE**	**RMSEr (%)**
September	−0.001	14	0.0107	35	0.0006	17	0.0058	29
October	−0.0004	−17	0.0079	11	0.0000	0	0.0052	7
November	−0.0002	11	0.0073	9	−0.0001	4	0.006	7
December	−0.0004	−9	0.0195	22	0.0004	1	0.0062	7
January	0.0000	−20	0.0073	8	0.0009	1	0.0113	13
February	−0.0219	−20	0.1318	134	0.0011	28	0.0084	14
March	−0.0095	−23	0.0721	149	−0.001	12	0.0367	126
April	−0.0016	−52	0.0082	239	0.0001	74	0.0013	79

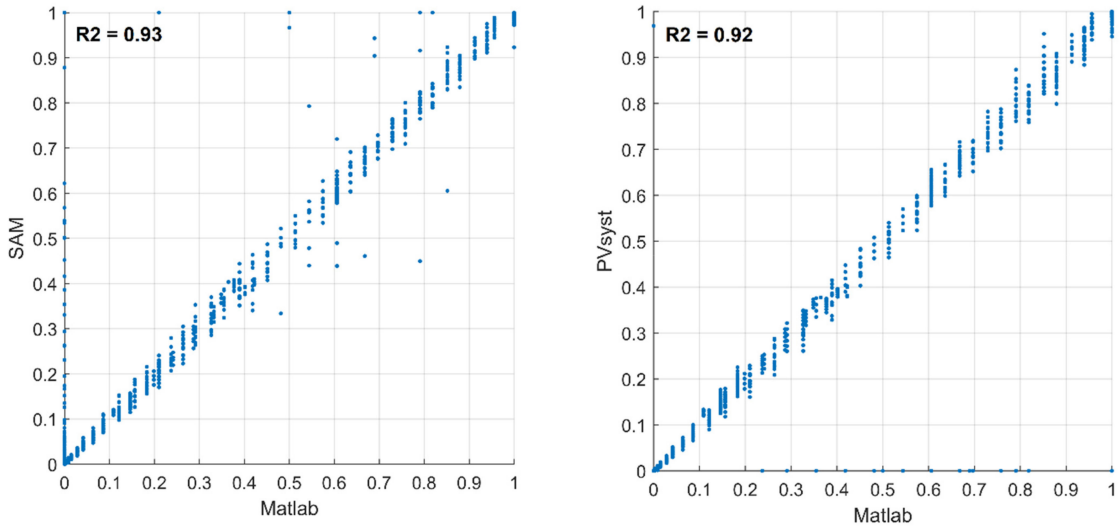

(**a**) (**b**)

Figure 19. Scatter plots for the direct irradiance shading factor f_B. Comparison of: (**a**) Matlab with SAM and (**b**) Matlab with PVsyst. Results are for situation 1, one module shaded by a single obstacle positioned on the east side.

Deviation parameters for situation 2 are shown in Table 4. Because in this situation the shading factors are zero from October to April, these months were excluded from the table. Again, the Matlab tool and SAM present similar results. However, PVsyst results differed significantly. The scatter plot of Figure 20 shows good correlation between Matlab and SAM. In this case, Matlab predicted slightly larger shading factors.

Table 4. Deviation parameters between the Matlab tool, SAM, and PVsyst for situation 2.

Infinite Row								
Month	**SAM**				**PVsyst**			
	MBE	**MBEr (%)**	**RMSE**	**RMSEr (%)**	**MBE**	**MBEr (%)**	**RMSE**	**RMSEr (%)**
April	0.005	89	0.021	118	0.002	35	0.013	159
May	0.008	88	0.024	57	0.004	54	0.015	62
June	0.008	40	0.021	54	0.005	18	0.015	34
July	0.006	60	0.016	49	0.004	41	0.012	41
August	0.003	33	0.015	38	0.004	68	0.021	181
September	−0.002	−29	0.032	1005	0.000	216	0.006	1768

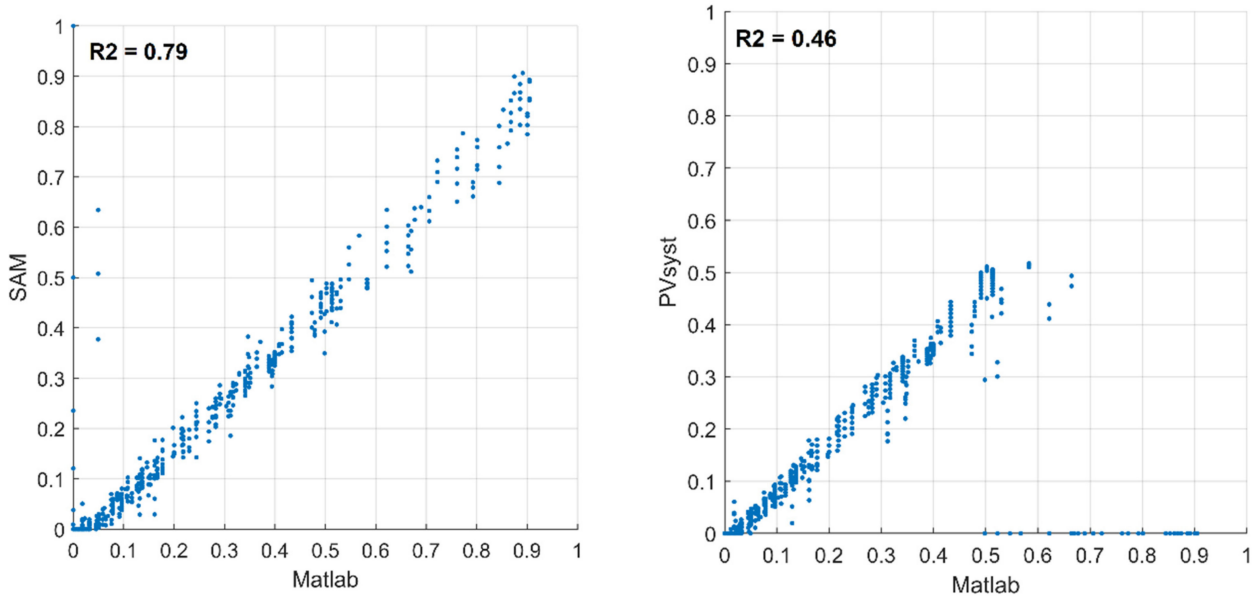

(**a**) (**b**)

Figure 20. Scatter plots for the direct irradiance shading factor f_B. Comparison of: (**a**) Matlab with SAM and (**b**) Matlab with PVsyst. Results are for situation 2, one module shaded by one infinite row.

The main reason for the discrepancies of PVsyst was the hourly time steps that PVsyst used to calculate the shading factors. This shows the importance of using smaller steps during calculations. Furthermore, these results were achieved using the "Slow calculation mode" for the lineal shading simulation tool of PVsyst. This mode calculates f_B for each time step and leads to relatively good results. The fast mode uses a pre-calculated shading table and can lead to greater discrepancies.

This is because the table has large steps of the azimuth and elevation angles. These angles are 20° and 10°, respectively.

3.2. Diffuse Irradiance Shading Factor

The diffuse shading factor is constant and needs to be calculated only once. To compare the model with SAM and PVsyst, we used the previously mentioned geometries. The only difference was that in this case, we varied the distance of separation d between the module and the obstacle (previously considered 2 m). This allowed a broader comparison. For the infinite row, f_D was calculated with different distances of separation between the module and the row in front. For the $1 \times 1 \times 5$ block, different distances from the module to the block were considered. These distances are shown in Figure 21.

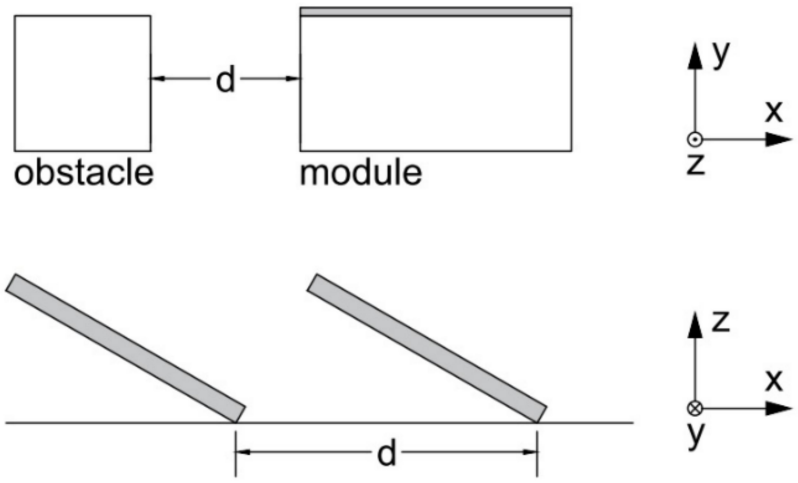

Figure 21. Geometry of the shading situations where *d* is a varied parameter.

Figures 22 and 23 show the diffuse shading factors for the situations described. Small discrepancies are observed. The proposed tool yielded good correlation with the results obtained in PVsyst. This suggests that our model and PVsyst use a similar approach during the calculation of the diffuse shading factor. Surprisingly, in the second situation, the results of SAM diverged significantly from both PVsyst and the Matlab tool for small distances of separation. One possible reason for this is that SAM uses a separate calculation procedure for self-shading losses [34]. Deviation parameters are shown in Tables 5 and 6 for situations 1 and 2, respectively.

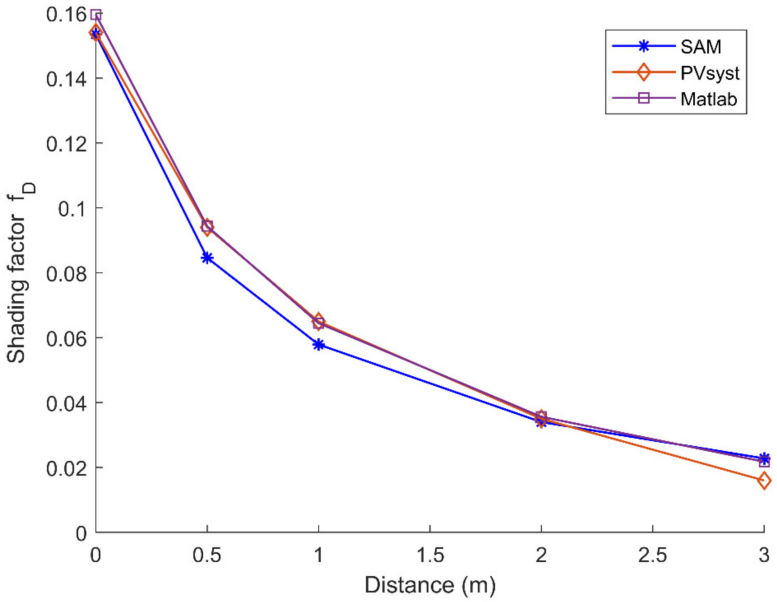

Figure 22. Diffuse shading factor for a module shaded by a block positioned on the east side of the module, assuming different distances of separation.

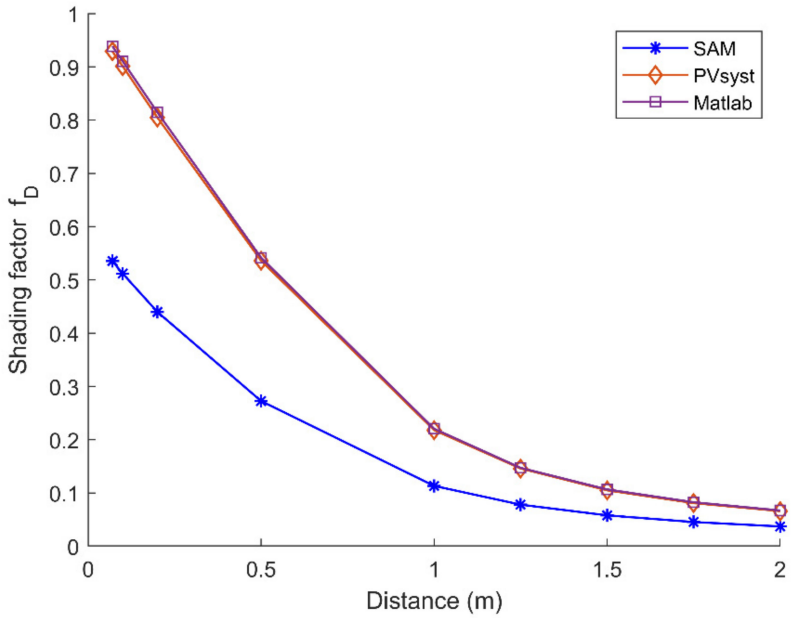

Figure 23. Diffuse shading factor for a module shaded by an infinite row, assuming different distances of separation.

Table 5. MBE for the diffuse shading factor f_D. East obstacle.

East Obstacle				
Distance (m)	**SAM**		**PVsyst**	
	MBE	**MBEr (%)**	**MBE**	**MBEr (%)**
0	0.0061	3.94	0.0056	3.61
0.5	0.0097	11.50	0.0003	0.35
1	0.0066	11.36	−0.0005	−0.80
2	0.0016	4.79	0.0006	1.80
3	−0.0010	−4.45	0.0058	36.16

Table 6. MBE for the diffuse shading factor f_D. Infinite row.

Infinite Row				
Distance (m)	**SAM**		**PVsyst**	
	MBE	**MBEr (%)**	**MBE**	**MBEr (%)**
0.07	0.4034	75.35	0.0098	1.06
0.1	0.3986	77.88	0.0094	1.04
0.2	0.3748	85.17	0.0098	1.21
0.5	0.2691	98.70	0.0057	1.06
1	0.1073	94.73	0.0026	1.21
1.25	0.0692	88.56	0.0013	0.87
1.5	0.0487	84.03	0.0017	1.66
1.75	0.0372	81.71	0.0017	2.07
2	0.0300	80.72	0.0012	1.86

4. Results

An array of PV modules was modeled. The proposed situation was an array with 3 rows and 5 columns, i.e., 15 modules, as shown in Figure 24. This situation also had one wall of 3 m height and situated at a distance of 2 m from the east-side column. Modules

had a tilt angle of 30° and an azimuth of 0°. The location was Mar del Plata (38° S, 57.5° W) and the time was the year 2020. With this method, a shading table for each module of the array could be calculated, as shown in Figure 25. Also, Figures 26 and 27 present the calculated direct shading factor f_B as a function of time and the diffuse shading factor f_D for each of the array's modules, respectively.

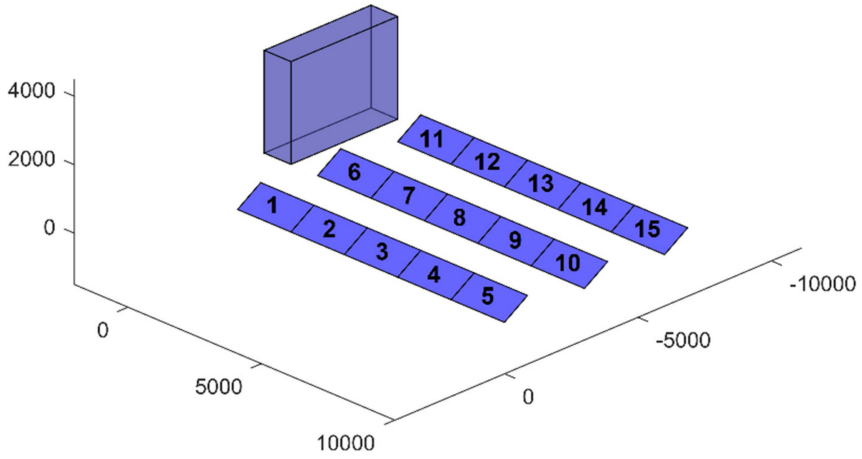

Figure 24. Proposed situation for calculating the shading tables of an array.

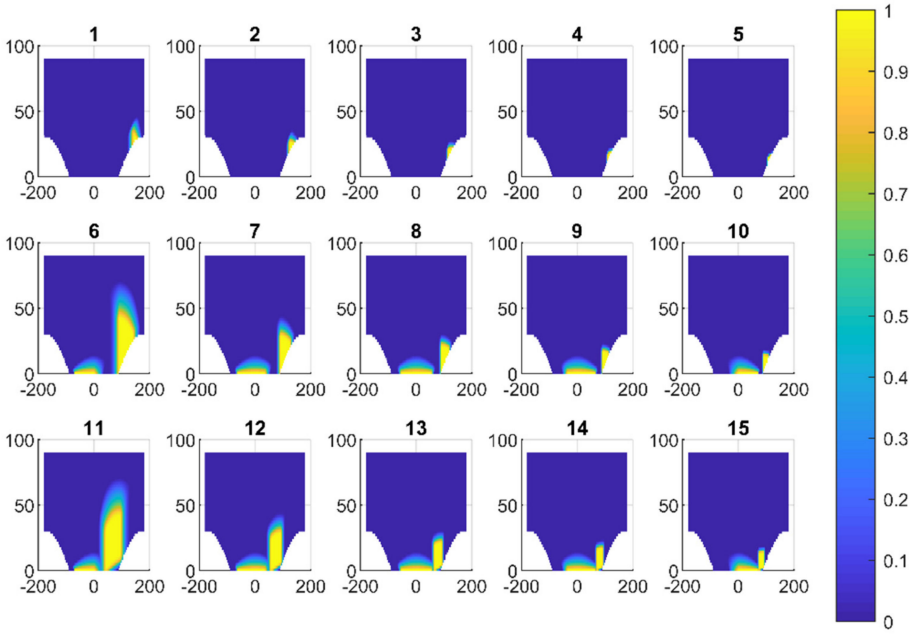

Figure 25. Shading tables for each of the modules in the array, represented as heat plots.

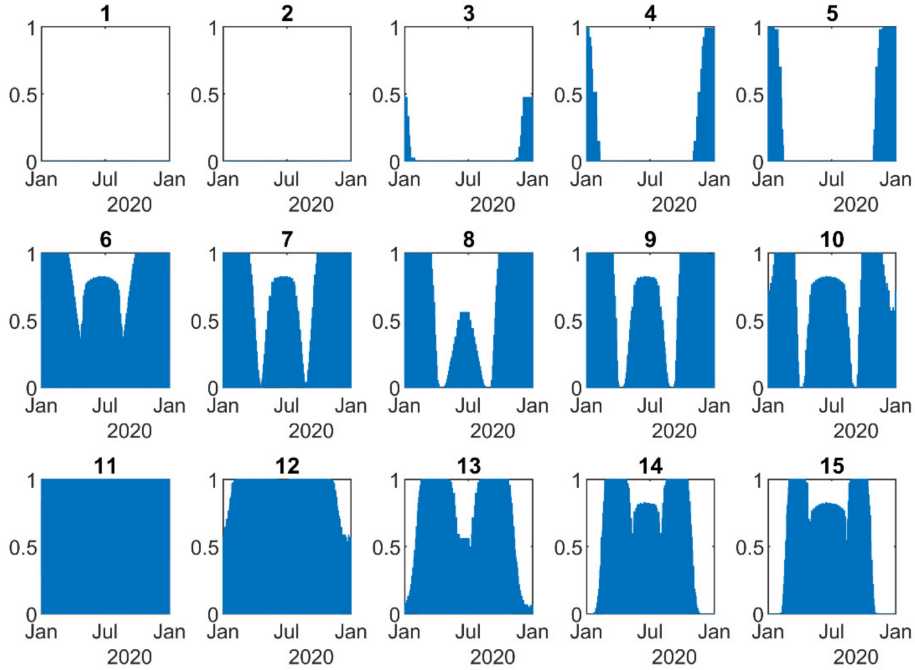

Figure 26. Direct shading factor f_B as a function of time for all the modules in the array.

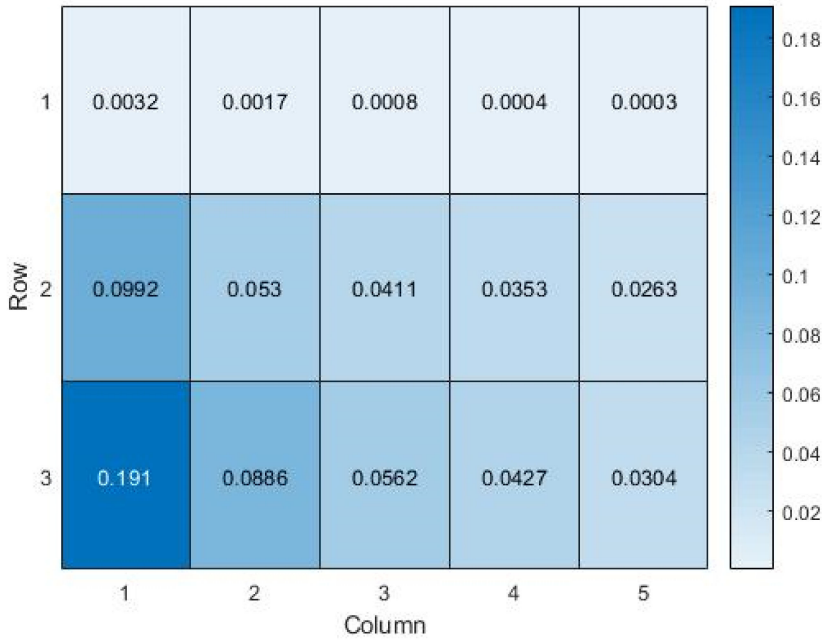

Figure 27. Diffuse shading factor f_D for all the modules in the array.

5. Conclusions

In this work, a Matlab-based procedure and a tool for estimating the shading factors were proposed. This method provides a means of including the effect of shadows in the direct and diffuse irradiances with Matlab. By setting the geometry of the module and the obstacle, a shading table can be calculated. This provides an easy way for retrieving the direct shading factor f_B and the diffuse shading factor f_D by the integration of the shading table.

The calculated shading factor for the direct irradiance f_B showed a good relationship with the values obtained with the software SAM. However, we observed larger discrep-

ancies when compared with the software PVsyst, mainly due to its hourly time steps. In this matter, we have shown the importance of small time steps when calculating accurate shading factors, and 5-min steps seem to achieve good results. In regard to the diffuse shading factor, the results obtained in Matlab correlated well with the results of PVsyst.

A key advantage of this work is that it provided more flexibility, control, and transparency over the shading factor calculation process. These characteristics make this Matlab tool an attractive option for the performance of research. Moreover, this could be a valuable addition to the PV_LIB library of Sandia Laboratories, which currently has no means for including shading effects. Finally, this tool is not limited to photovoltaic systems; it also may be applied to every situation where an irradiance reduction must be considered.

Any reader interested in obtaining the Toolbox source code can contact the corresponding author.

Author Contributions: Conceptualization, methodology, software and writing—original draft preparation, M.S.; writing—review and editing, J.J.R.; supervision, P.O.P. All authors have read and agreed to the published version of the manuscript.

Funding: This research received no external funding.

Institutional Review Board Statement: Not applicable.

Informed Consent Statement: Not applicable.

Data Availability Statement: Not applicable.

Acknowledgments: The authors are thankful to the LEyDE laboratory from the UNMdP who facilitated the experimental data from the PV system to be used in the present research.

Conflicts of Interest: The authors declare no conflict of interest.

Nomenclature

The following nomenclature is used in this manuscript:

f_B	Shading factor for direct irradiance
f_D	Shading factor for diffuse irradiance
DNI	Direct normal Irradiance
DHI	Diffuse horizontal Irradiance
A_S	Shaded area of the solar module
A_M	Area of the module
v_i	Vertices of each corner of the module
β	Tilt angle of the module
γ	Azimuth angle of the module
R_y	Rotation matrix about the y axis
R_z	Rotation matrix about the z axis
p_0	Obstacle vertex
p_s	Projection of the obstacle vertex on the plane of the module
a	Vector normal to the module plane
s	Unit vector with the sun position in Cartesian coordinates
I_S	Irradiance traversing the shaded area AS (diffuse)
I_H	Irradiance reaching the area of the hemisphere AH (diffuse)
R	Radiance of a sky element
AOI	Angle of incidence
α	Elevation angle of the sun

References

1. Green, M.A. Commercial progress and challenges for photovoltaics. *Nat. Energy* **2016**, *1*, 15015. [CrossRef]
2. Eigensonne Das 1000 Dächer Programm. Available online: https://www.eigensonne.de/1000-daecher-programm/ (accessed on 22 October 2020).
3. Strahs, G.; Tombari, C. *Laying the Foundation for a Solar America: The Million Solar Roofs Initiative*; National Renewable Energy Lab. (NREL): Golden, CO, USA, 2006. [CrossRef]

4. North Carolina Federal Ministry of the Environment; N.S. (BMU) 100.000 Dächer-Solarstrom-Programm. Available online: https://www.bmu.de/pressemitteilung/100000-daecher-solarstrom-programm-kurz-vor-dem-ziel/ (accessed on 1 November 2020).
5. Enkhardt, S. Österreichs 1-Million-Dächer-Programm für Photovoltaik nimmt Formen an. Available online: https://www.pv-magazine.de/2020/09/10/oesterreichs-1-million-daecher-programm-fuer-photovoltaik-nimmt-formen-an/ (accessed on 22 October 2020).
6. Fraunhofer Institute for Solar Energy Systems (ISE). Photovoltaics Report. Available online: https://www.ise.fraunhofer.de/content/dam/ise/de/documents/publications/studies/Photovoltaics-Report.pdf (accessed on 16 September 2020).
7. Ellabban, O.; Abu-Rub, H.; Blaabjerg, F. Renewable energy resources: Current status, future prospects and their enabling technology. *Renew. Sustain. Energy Rev.* **2014**, *39*, 748–764. [CrossRef]
8. Decker, B.; Jahn, U. Performance of 170 grid connected PV plants in Northern Germany—Analysis of yields and optimization potentials. *Sol. Energy* **1997**, *59*, 127–133. [CrossRef]
9. Quaschning, V.; Hanitsch, R. Irradiance calculation on shaded surfaces. *Sol. Energy* **1998**, *62*, 369–375. [CrossRef]
10. MacAlpine, S.; Deline, C.; Dobos, A. Measured and estimated performance of a fleet of shaded photovoltaic systems with string and module-level inverters. *Prog. Photovolt. Res. Appl.* **2017**, *25*, 714–726. [CrossRef]
11. Bayrak, F.; Ertürk, G.; Oztop, H.F. Effects of partial shading on energy and exergy efficiencies for photovoltaic panels. *J. Clean. Prod.* **2017**, *164*, 58–69. [CrossRef]
12. Numan, A.H.; Dawood, Z.S.; Hussein, H.A. Theoretical and experimental analysis of photovoltaic module characteristics under different partial shading conditions. *Int. J. Power Electron. Drive Syst.* **2020**, *11*, 1508–1518. [CrossRef]
13. Quaschning, V.; Hanitsch, R. Shade Calculations in Photovoltaic Systems. In Proceedings of the ISES Solar World Conference, Harare, Zimbabwe, 11–15 September 1995; pp. 1–5.
14. Haberlin, H. *Photovoltaics: System Design and Practice*; John Wiley & Sons, Ltd.: Chichester, UK, 2012; ISBN 9781626239777.
15. Teo, J.C.; Tan, R.H.G.; Mok, V.H.; Ramachandaramurthy, V.K.; Tan, C. Impact of Partial Shading on the P-V Characteristics and the Maximum Power of a Photovoltaic String. *Energies* **2018**, *11*, 1860. [CrossRef]
16. MacAlpine, S.; Deline, C. Simplified method for modeling the impact of arbitrary partial shading conditions on PV array performance. In Proceedings of the IEEE 42nd Photovoltaic Specialist Conference (PVSC), New Orleans, LA, USA, 14–19 June 2015; pp. 1–6. [CrossRef]
17. Cascone, Y.; Corrado, V.; Serra, V. Calculation procedure of the shading factor under complex boundary conditions. *Sol. Energy* **2011**, *85*, 2524–2539. [CrossRef]
18. Melo, E.G.; Almeida, M.P.; Zilles, R.; Grimoni, J.A. Using a shading matrix to estimate the shading factor and the irradiation in a three-dimensional model of a receiving surface in an urban environment. *Sol. Energy* **2013**, *92*, 15–25. [CrossRef]
19. Westbrook, O.; Reusser, M.; Collins, F. Diffuse shading losses in tracking photovoltaic systems. In Proceedings of the IEEE 40th Photovoltaic Specialist Conference (PVSC), Denver, CO, USA, 8–13 June 2014; pp. 0891–0896. [CrossRef]
20. Li, Y.; Ding, D.; Liu, C.; Wang, C. A pixel-based approach to estimation of solar energy potential on building roofs. *Energy Build.* **2016**, *129*, 563–573. [CrossRef]
21. National Reneable Energy Laboratory (NREL). System Advisor Model (SAM). Available online: https://sam.nrel.gov/ (accessed on 1 January 2021).
22. PVsyst, S.A. PVsyst. Available online: https://www.pvsyst.com/ (accessed on 20 March 2021).
23. Valentin Software PV*SOL. Available online: https://valentin-software.com/en/products/pvsol/ (accessed on 1 March 2021).
24. Folsom Labs Helioscope. Available online: https://www.helioscope.com/ (accessed on 1 January 2021).
25. Sandia National Laboratories. PV_LIB Toolbox. Available online: https://pvpmc.sandia.gov/applications/pv_lib-toolbox/ (accessed on 20 May 2020).
26. Trejos Grisales, L.A.; Ramos Paja, C.A.; Saavedra Montes, A.J. Techniques for modeling photovoltaic systems under partial shading. *Tecnura* **2016**, *20*, 171–183. [CrossRef]
27. PVsyst Shading Factor Table. Available online: https://www.pvsyst.com/help/shadings_factor_table.htm (accessed on 17 September 2020).
28. Evans, P.R. Rotations and rotation matrices. *Acta Crystallogr. Sect. D Biol. Crystallogr.* **2001**, *57*, 1355–1359. [CrossRef] [PubMed]
29. University of Texas. Equations of Planes. Available online: https://web.ma.utexas.edu/users/m408m/Display12-5-3.shtml (accessed on 4 July 2021).
30. The MathWorks. Convhull. Available online: https://www.mathworks.com/help/matlab/ref/convhull.html (accessed on 21 October 2020).
31. The MathWorks. Polyshape. Available online: https://www.mathworks.com/help/matlab/ref/polyshape.html?s_tid=doc_ta (accessed on 9 February 2020).
32. The MathWorks. Intersect. Available online: https://www.mathworks.com/help/matlab/ref/double.intersect.html?s_tid=doc_ta (accessed on 15 February 2021).
33. Sandia National Laboratories. Angle of Incidence. Available online: https://pvpmc.sandia.gov/modeling-steps/1-weather-design-inputs/plane-of-array-poa-irradiance/calculating-poa-irradiance/angle-of-incidence/ (accessed on 9 February 2020).
34. Gilman, P. SAM Photovoltaic Model Technical Reference SAM Photovoltaic Model Technical Reference. *Sol. Energy* **2015**, *63*, 323–333. [CrossRef]